J. Plasma Physics (2002), *vol.* 67, *part* 4, *pp.* 223–233. © 2002 Cambridge University Press 223
DOI: 10.1017/S0022377801001404 Printed in the United Kingdom

Anomalous width variation for rarefactive ion acoustic solitary waves in the presence of warm multi-ions

S. S. GHOSH[1]* and A. N. SEKAR IYENGAR[2]

[1]Department of Electronic and Electrical Engineering, Pohang University of Science and Technology, Pohang, 790 784, Republic of Korea (sukti@postech.ac.kr)

[2]Saha Institute of Nuclear Physics, 1/AF Bidhannagar, Calcutta, 700 064 India (iyengar@hp2.saha.ernet.in)

(Received 21 June 2001)

Abstract. A previous analysis of anomalous width variation for a single-ion rarefactive solitary wave [S. S. Ghosh and A. N. Sekar Iyengar, *Phys. Plasmas*, **4**, 3204 (1997)] has been extended to a multi-ion species, and shows that the corresponding width–amplitude characteristics depend crucially on the respective ion concentrations; for example, with increasing light-ion concentration, an 'increasing-width' rarefactive solitary wave transforms to a 'decreasing-width' one for a constant Mach number exhibiting an overall U-shaped variation profile. The influence of the second ion species generally decreases with increasing amplitude, being maximum for the single to multi-ion transition. However, in the neighbourhood of double-layer-like solutions, the influence again becomes prominent, which may be associated with the corresponding energy–amplitude relations for both the ions.

1. Introduction

In our previous work, we have studied in detail the properties of a rarefactive solitary wave for a two-electron-temperature plasma containing a single warm ion species. The corresponding amplitude–width variation has exhibited three distinct regions: regions I (small amplitude, decreasing width), II (intermediate amplitude, near constant width) and III (large amplitude, increasing width) (Ghosh et al. 1996; Ghosh and Iyengar 1997b). It is well known that a rarefactive solitary wave transforms to weak double layers (Böstrom et al. 1988). Böstrom et al. (1989) previously indicated that such rarefactive solitary waves do not follow the Korteweg–de Vries (KdV) type of width–amplitude variation. This is further supported by our theoretical investigations of anomalous width variations (region III) (Ghosh and Iyengar 1997b), which in turn transform to double layers. Such a transition thus appears to be closely correlated with existing space plasma observations (Berthomier et al. 1998). So far we have confined ourselves to only a single ion species. However, there are many cases of practical importance where a plasma may contain impurities (Kadomtsev 1992; Buti 1983). This motivates us to study the influence of the

* Present address: Indian Institute of Geomagnetism, Dr Nanabhai Moos Marg, Colaba, Mumbai, 400 005 India.

presence of multi-ions on the anomalous width variation. It is observed that the respective ion densities have a profound effect on the corresponding width–amplitude variation profile, and also modify it qualitatively.

In Sec. 2, we derive the exact analytical form of the Sagdeev pseudopotential for a warm multi-ion plasma containing two-temperature electrons. In Secs 3.1 and 3.2, we investigate the effects of ion concentrations and mass ratio on the width–amplitude characteristics of the rarefactive solitary wave. In Sec. 3.3, we present the influence of the multi-ion species on general parametric variations. Finally, Sec. 4 contains our concluding remarks.

2. Analytical methods

We start with the usual warm-ion (adiabatic) fluid equations (Ghosh et al. 1996) for ions of two different masses for an infinite one-dimensional collisionless unmagnetized plasma:

$$\frac{\partial n_{ih}}{\partial t} + \frac{\partial (n_{ih} v_{ih})}{\partial x} = 0, \tag{2.1a}$$

$$\frac{\partial n_{il}}{\partial t} + \frac{\partial (n_{il} v_{il})}{\partial x} = 0, \tag{2.1b}$$

$$\frac{\partial v_{ih}}{\partial t} + v_{ih}\frac{\partial v_{ih}}{\partial x} + \frac{\sigma_{\text{eff}}}{n_{ih}}\frac{\partial p_{ih}}{\partial x} = -\frac{\partial \phi}{\partial x}, \tag{2.1c}$$

$$\frac{\partial v_{il}}{\partial t} + v_{il}\frac{\partial v_{il}}{\partial x} + Q\frac{\sigma_{\text{eff}}}{n_{il}}\frac{\partial p_{il}}{\partial x} = -Q\frac{\partial \phi}{\partial x}, \tag{2.1d}$$

$$\frac{\partial p_{ih}}{\partial t} + v_{ih}\frac{\partial p_{ih}}{\partial x} + 3p_{ih}\frac{\partial v_{ih}}{\partial x} = 0, \tag{2.1e}$$

$$\frac{\partial p_{il}}{\partial t} + v_{il}\frac{\partial p_{il}}{\partial x} + 3p_{il}\frac{\partial v_{il}}{\partial x} = 0, \tag{2.1f}$$

with

$$\sigma_{\text{eff}} = \frac{T_i}{T_{\text{eff}}} = \alpha_h\sigma_h + \alpha_l\sigma_l, \qquad T_i = \alpha_h T_{ih} + \alpha_l T_{il}, \qquad T_{\text{eff}} = \frac{T_{ec}T_{ew}}{\mu T_{ew} + \nu T_{ec}}.$$

The corresponding Poisson equation is

$$\frac{\partial^2 \phi}{\partial x^2} = n_{ec} + n_{ew} - n_{ih} - n_{il}, \tag{2.2}$$

with

$$n_e = n_c + n_h = \mu e^{\phi/(\mu+\nu\beta)} + \nu e^{\beta\phi/(\mu+\nu\beta)}. \tag{2.3}$$

The subscripts i, e, c, w, h and l refer to ions, electrons, cold and warm electrons, and heavy and light ions respectively, while σ_k $(= T_{ik}/T_{\text{eff}};\ k = h, l)$, β $(= T_{ec}/T_{ew})$ and Q $(= m_{ih}/m_{il})$ are the finite-ion-temperature effect, the cold-to-hot electron temperature ratio and the heavy-to-light ion mass ratio respectively, with the remaining notation having its usual meaning. All the number densities, namely μ, ν, α_h and α_l, which are the initial densities for cold and warm electrons and heavy and light ions respectively, are normalized to the equilibrium plasma density n_0 $(\mu + \nu = \alpha_h + \alpha_l = 1)$, the ion pressure p_{ik} $(k = h, l)$ is normalized to the ion equilibrium pressure p_0 $(= n_0 T_i)$, and the other variables t, x, v_i and ϕ are normalized to the reciprocal ion plasma frequency ω_{pi}^{-1} $(\omega_{pi} = \sqrt{4\pi n_0 e^2/m_{ih}})$, the effective Debye

https://doi.org/10.1017/S0022377801001404 Published online by Cambridge University Press

length λ_{eff} $(=\sqrt{T_{\text{eff}}/4\pi n_0 e^2})$, the effective ion acoustic velocity v_{eff} $(=\sqrt{T_{\text{eff}}/m_{ih}})$ and T_{eff}/e respectively. The Mach number M is also normalized by v_{eff}. For all the cases, we have used the heavy-ion mass as the normalization parameter.

We assume the following normalized boundary conditions:

$$v_{ik} \to v_0, \quad \sum p_{ik} \to 1, \quad \sum n_{ik} \to 1, \quad \phi \to 0 \quad \text{as } |x| \to \infty, \tag{2.4a}$$

which also imply that

$$p_{ik} \to \alpha_k \frac{\sigma_k}{\sigma_{\text{eff}}}, \qquad n_{ik} \to \alpha_k \qquad \text{as } |x| \to \infty. \tag{2.4b}$$

Solving these fluid equations in a stationary-wave frame, we obtain the corresponding warm-ion densities as

$$n_{ih} = \frac{\alpha_h}{2\sqrt{3\sigma_h}} \left\{ [(M+\sqrt{3\sigma_h})^2 - 2\phi]^{1/2} - [(M-\sqrt{3\sigma_h})^2 - 2\phi]^{1/2} \right\}, \tag{2.5a}$$

$$n_{il} = \frac{\alpha_l}{2\sqrt{3\sigma_l}} \left\{ \left[\left(\frac{M}{\sqrt{Q}} + \sqrt{3\sigma_l} \right)^2 - 2\phi \right]^{1/2} - \left[\left(\frac{M}{\sqrt{Q}} - \sqrt{3\sigma_l} \right)^2 - 2\phi \right]^{1/2} \right\}. \tag{2.5b}$$

Integrating the Poisson equation with these ion densities, we obtain the required form of the pseudopotential as

$$\begin{aligned}
\psi(\phi) = -\Bigg\{ & (\mu+\nu\beta) \left[\mu(e^{\phi/(\mu+\nu\beta)} - 1) + \frac{\nu}{\beta}(e^{\beta\phi/(\mu+\nu\beta)} - 1) \right] \\
& + \frac{\alpha_h}{6\sqrt{3\sigma_h}} \Big\{ [(M+\sqrt{3\sigma_h})^2 - 2\phi]^{3/2} - (M+\sqrt{3\sigma_h})^3 \\
& - [(M-\sqrt{3\sigma_h})^2 - 2\phi]^{3/2} + (M-\sqrt{3\sigma_h})^3 \Big\} \\
& + \frac{\alpha_l}{6\sqrt{3\sigma_l}} \left\{ \left[\left(\frac{M}{\sqrt{Q}} + \sqrt{3\sigma_l} \right)^2 - 2\phi \right]^{3/2} - \left(\frac{M}{\sqrt{Q}} + \sqrt{3\sigma_l} \right)^3 \right. \\
& \left. - \left[\left(\frac{M}{\sqrt{Q}} - \sqrt{3\sigma_l} \right)^2 - 2\phi \right]^{3/2} + \left(\frac{M}{\sqrt{Q}} - \sqrt{3\sigma_l} \right)^3 \right\} \Bigg\}.
\end{aligned} \tag{2.6}$$

For simplicity, unless otherwise specified, we shall consider equal ion temperatures for the two species, i.e. $\sigma = \sigma_h = \sigma_l$.

This Sagdeev pseudopotential, when it satisfies the required boundary conditions (Ghosh et al. 1996), leads to a solitary-wave solution. These conditions on $\psi(\phi)$ (Ghosh et al. 1996) also predict the limiting value of the Mach number M for a solitary wave. The existence of a solitary-wave solution is thus implied by the following inequality:

$$\frac{\alpha_h}{M^2 - 3\sigma_h} + \frac{\alpha_l}{(M^2/Q) - 3\sigma_l} < 1. \tag{2.7}$$

Equation (2.7) is the boundary condition for M. It also implies that the limiting value of M depends on the parameters Q, α_h and σ_k $(k = h, l)$. Since it is of fourth

https://doi.org/10.1017/S0022377801001404 Published online by Cambridge University Press

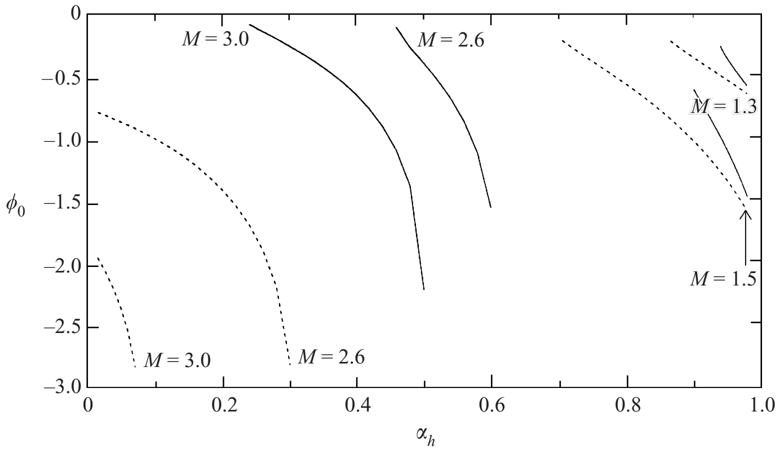

Figure 1. Variation of amplitude with ion concentration α_h for different values of M, with $\sigma = \frac{1}{30}$, $\mu = 0.15$, $\beta = \frac{1}{40}$ and $Q = 4$ (dashed curves) and 10 (solid curves).

order, it is not possible to get any explicit relationship for M. For cold ions ($\sigma_k = 0$), this condition reduces to that derived by White et al. (1972), and for $Q = 1$, $\sigma \neq 0$, it reduces to the modified Bohm criterion for a warm single ion.

3. Anomalous width variation

In order to investigate the effect of the second ion species, we investigate the solitary-wave solutions for different α_h and Q. Unless otherwise specified, the other parameters μ, β and σ are kept constant. In all the cases, the Mach number is normalized by the ion acoustic speed of the heavy ions.

3.1. Effect of α_h

In Fig. 1, we have plotted the variation of the amplitude for a rarefactive solitary wave for different M assuming two different mass ratios $Q = 4$ and 10. It shows that an increase in the light-ion concentration (decrease in α_h) produces a sharp decrease in the rarefactive solitary-wave amplitude; for example, for $Q = 10$, even a 10% light-ion impurity is enough to inhibit the solitary-wave formation owing to the rapid decrease in amplitude, provided that the Mach number is kept constant. However, as Q is decreased, this restriction is relaxed to a great extent; for example, rarefactive solitary waves with light-ion concentration as large as 30% have been obtained for $Q = 4$ and $M = 1.5$. On the other hand, in a light-ion-dominated plasma, the heavy-ion impurity produces a rapid increase in amplitude, and the rarefactive solitary-wave terminates in a double-layer solution; for example, for $Q = 4$ and $M = 3$ ($M^* = M/\sqrt{Q} = 1.5$), only 8% of heavy-ion impurity is sufficient to terminate the solitary-wave solution. This effect is expected to increase with increasing mass ratio. Rarefactive solitary waves in an intermediate plasma, having a comparable amount of both light and heavy ions, are bounded by both lower and upper limits of heavy-ion concentrations; for example, for $Q = 10$ and $M = 2.6$, the rarefactive solitary wave is bounded between $0.45 \geqslant \alpha_h \geqslant 0.6$. This α_h variation further indicates that a rarefactive solitary wave may have different characteristics for different ranges of heavy-ion concentrations, namely heavy-ion-dominated

https://doi.org/10.1017/S0022377801001404 Published online by Cambridge University Press

($\alpha_h \geqslant 0.8$), intermediate ($0.4 \leqslant \alpha_h \leqslant 0.8$) and light-ion-dominated ($\alpha_h \leqslant 0.4$) plasmas.

The crucial dependence of the amplitude and the domain of existence on the impurity concentration is also found to influence the process of anomalous width variation. Figures 2(a) and (b) show the variation of W^2 with α_h for different M for the overall spectrum of the heavy-ion concentration. They indicate that for a heavy-ion-dominated plasma, the width generally decreases with α_h, while for a light-ion-dominated one, it increases. For an intermediate plasma, the width is minimum, and may show a minimum variation for an appreciable range of α_h, depending upon the choice of Mach number. The overall variation thus appears as a U-shaped profile, which is most prominent for an intermediate range of α_h, whereas its left or right arm diminishes and disappears as α_h approaches 0 or 1 respectively. Recalling that the amplitude always increases with α_h, we may conclude that the left arm of the 'U' profile corresponds to a 'decreasing-width' solitary wave (region I; small-amplitude solutions), while the right arm is the 'increasing-width' or the anomalous region (region III; large-amplitude solutions), the base of the profile with the minimum width being the 'near-constant-width' region (region II) for a solitary wave with intermediate amplitude. The shape of these 'U' profiles may be quite narrow (e.g. $M = 2.2$, $Q = 10$) or appreciably extended (e.g. $M = 1.7$, $Q = 4$), depending upon the particular combination of M, Q and α_h, and generally becomes broadened with increasing M; for example, in Fig. 2(b) ($Q = 10$), the extent of the profile broadens as M increases from 2.2 to 3.0. These profiles reveal that the anomaly in the width variation for a rarefactive solitary wave depends crucially on the heavy-ion concentration. Increase in α_h beyond some threshold limit, particular for that parametric combination, will transform a 'decreasing-width' solitary wave to an 'increasing-width' one, or vice versa, which also indicates a qualitative change in the solitary-wave solution due to variation in the impurity ion concentration.

In Ghosh and Iyengar (1997b), we observed that the ion energy–amplitude relationship has some interesting consequences on the anomalous width variation. Analogously to the single-ion case, inclusion of finite ion temperature produces two energy components for each species of ions (Ghosh and Iyengar 1997a), namely

$$H_h = \tfrac{1}{2}(M + \sqrt{3\sigma})^2, \qquad L_h = \tfrac{1}{2}(M - \sqrt{3\sigma})^2$$

and

$$H_l = \frac{1}{2}\left(\frac{M}{\sqrt{Q}} + \sqrt{3\sigma}\right)^2, \qquad L_l = \frac{1}{2}\left(\frac{M}{\sqrt{Q}} - \sqrt{3\sigma}\right)^2,$$

thus producing two extra components compared with the single-ion case. The subscripts h (l) denote the heavy (light) ions for both the high-energy (H) and low-energy (L) components respectively. The role of all these four energy components regarding the energy–amplitude relations associated with the anomalous width variation is summarized in Table 1 for different values of α_h, describing a heavy-ion-dominated, intermediate or light-ion-dominated plasma. The mass ratio is assumed to be a constant ($Q = 10$).

Table 1 clearly indicates the association of the energy–amplitude relationship with a large-amplitude solution. Both the L (H) components of heavy (light) ions, namely L_h (H_l) respectively, show 'trapping'-like conditions (kinetic energy > potential energy), associated with the large-amplitude solutions, while the other two components, namely the H (L) components of the heavy (light) ions (H_h and

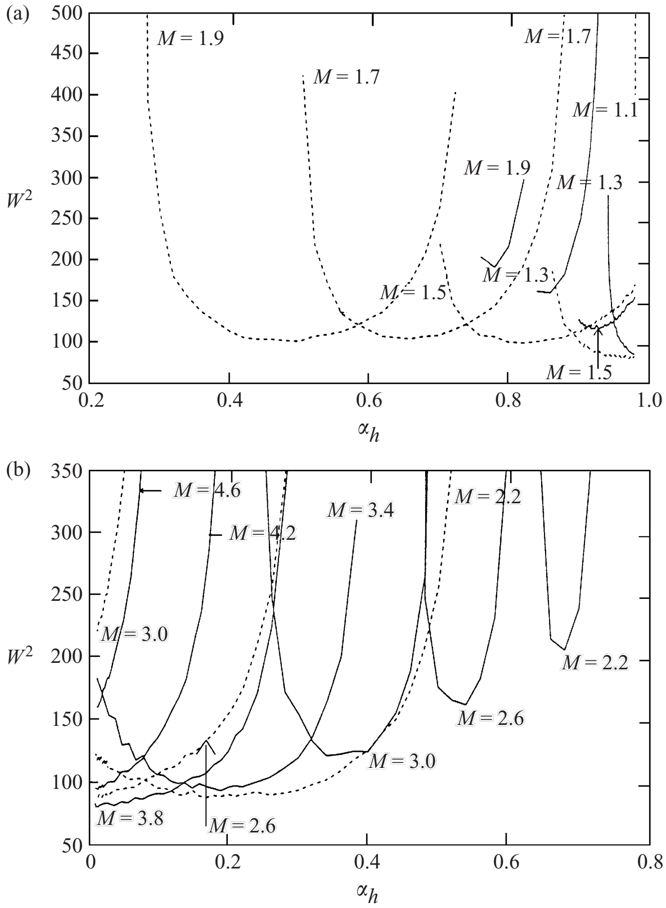

Figure 2. Parametric variation of width with α_h for different values of M, with $\sigma = \frac{1}{30}$, $\mu = 0.15$, $\beta = \frac{1}{40}$ and $Q = 4$ (dashed curve) and 10 (solid curves).

L_l respectively) remain unchanged because of their too large (small) kinetic energy compared to the amplitude. For a heavy-ion-dominated plasma, light ions have comparatively much smaller energies, i.e. $H_l < L_h$. With increasing mass ratio, their energies become even smaller, and the transition of the solitary wave solutions from the 'decreasing' to the 'increasing' width region is mainly associated with the heavy-ion energy (L_h). However, for a moderately large mass ratio ($Q = 10$), both L_h and H_l have comparable energies and participate in the width variation in a similar way. On the other hand, in a light-ion-dominated plasma, both the energy components of the heavy ions (i.e. H_h and L_h respectively) have much larger energies, and the anomalous width variation almost entirely depends upon the light ions. This is also consistent with our study of potential and density profiles (Ghosh and Iyengar 1997b) for different multi-ion plasmas. It shows that in a light-ion-dominated plasma, the heavy-ion impurities make little contribution to the overall density perturbations, while both species play significant roles in a small-amplitude solution for a heavy-ion-dominated plasma. However, the heavy ions seem to play a more dominating role, especially for large-amplitude solutions.

Table 1. The ion energy–amplitude relationships for different α_h.

	α_h	Energy relations	
		Region I	Region III
Heavy-ion-dominated plasma	0.98	$H_h > \phi_0$ $L_h > \phi_0$, $H_l \approx \phi_0$ $L_l < \phi_0$	$H_h \geqslant \phi_0$ $L_h < \phi_0$, $H_l < \phi_0$ $L_l < \phi_0$
Intermediate plasma	0.6	$H_h > \phi_0$ $L_h > \phi_0$, $H_l > \phi_0$ $L_l < \phi_0$	$H_h > \phi_0$ $L_h > \phi_0$, $H_l < \phi_0$ $L_l < \phi_0$
Light-ion-dominated plasma	0.15	$H_h \gg \phi_0$ $L_h > \phi_0$, $H_l > \phi_0$ $L_l > \phi_0$	$H_h \gg \phi_0$ $L_h > \phi_0$, $H_l \geqslant \phi_0$ $L_l < \phi_0$

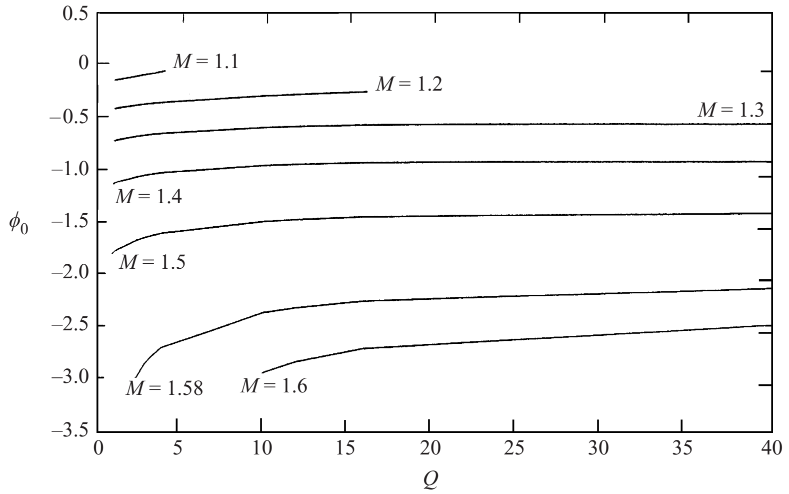

Figure 3. Variation of amplitude with mass ratio Q for different values of M, with $\alpha_h = 0.98$, $\sigma = \frac{1}{30}$, $\mu = 0.15$ and $\beta = \frac{1}{40}$.

3.2. Effect of Q

All the above analyses indicate a significant quantitative effect of mass ratio Q on the solitary-wave solution. Figure 3 shows the variation of the amplitude with the mass ratio Q for different M for a heavy-ion-dominated plasma ($\alpha_h = 0.98$), which reveals the expected decrease in amplitude in the presence of multi-ions. The rate of decrease is quite appreciable initially (i.e. when Q is close to 1), but reduces for a large mass ratio (e.g. $Q > 20$). The effect also depends on the parameter space (Mach number), being largest for a large Mach number (e.g. $M \geqslant 1.5$) and lowest for an intermediate range (e.g. $M \approx 1.3$). However, compared with the effect of the ion concentration (Fig. 1), the effect of the mass ratio on the amplitude variation is much less predominant.

Figure 4 shows the variation of W^2 with the mass ratio Q for different M. It shows that, for a small-amplitude solution ($M \leqslant 1.2$), the width increases for a multi-ion plasma (increasing mass ratio), while for a large-amplitude solution ($M \geqslant 1.58$), it decreases. For an intermediate amplitude ($1.3 \geqslant M \geqslant 1.5$), the width remains almost constant. The dependence of the width on the mass ratio is analogous to

https://doi.org/10.1017/S0022377801001404 Published online by Cambridge University Press

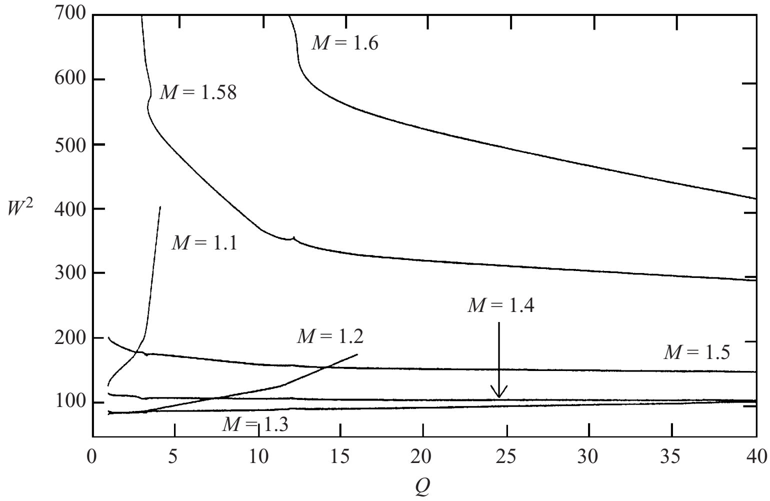

Figure 4. Parametric variation of W^2 with Q for different values of M, with $\alpha_h = 0.98$, $\sigma = \frac{1}{30}$, $\mu = 0.15$ and $\beta = \frac{1}{40}$.

that on the ion temperature, as observed in Ghosh and Iyengar (1997b), which probably indicates that the parameters σ and Q play similar roles in the width behaviour of the rarefactive solitary-wave solution. However, the effect of α_h on a rarefactive solitary wave remain distinctly different, both quantitatively (e.g. the amplitude variation; Fig. 1) and qualitatively (e.g. the width variation; Fig. 2), which contradicts the previously existing idea (Baboolal et al. 1990) that Q and α_h play similar roles analogous to that of the ion temperature σ for rarefactive solitary-wave solutions. Further comparisons with the single-ion case (Ghosh and Iyengar 1997b) reveal that both electron and ion concentrations determine the width–amplitude variation pattern qualitatively, while both the ion temperature and the ion mass ratio produce small quantitative changes by reducing the wave amplitude.

The inclusion of the second ion species also influences the existence domain of the corresponding rarefactive solitary-wave solutions. Figure 5 shows the variations of both M_{min} and M_{max} with α_h for two different mass ratios, $Q = 10$ and 4. The shaded regions are the corresponding domains of existence, while $\alpha_h = 1$ shows the allowed Mach number range for a single-ion (Ar) plasma. In a light-ion-dominated plasma, the large increase in the lower bound of the Mach number (i.e. $M > 3$) is mainly due to our particular choice of normalization (i.e. heavy-ion normalization).

3.3. Effect of σ, β and μ

To complete our discussion, we have plotted ϕ_r $(= \phi_{0\text{multi}}/\phi_{0\text{single}})$ with respect to different parameters, σ, μ and β in Figs. 6, 7 and 8 respectively. In all the cases, α_h $(= 0.98)$ and Q $(= 10)$ are kept constant. The variation of ϕ_r measures the deviation due to the presence of multi-ions, $\phi_r = 1$ being the single-ion case. In all the cases, the effect of the multi-ion species is maximum for a small-amplitude solution, and decreases with increasing amplitude (i.e. increasing M, μ and β and decreasing σ). However, in the neighbourhood of the double-layer-like solutions, the effect starts to increase. Figure 6 shows an increase in the deviation of ϕ_r for large M $(= 1.5)$, while Fig. 7 shows the same beyond a certain threshold value of μ. Figure 8 shows

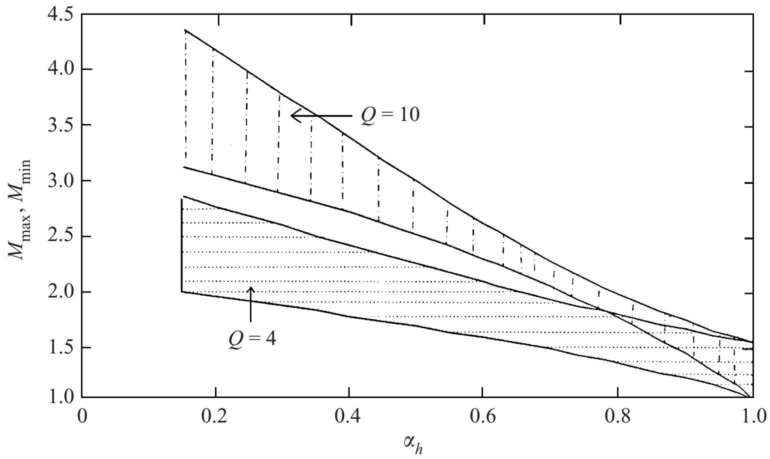

Figure 5. Domain of existence for a rarefactive solitary wave in a multi-ion plasma with $\sigma = \frac{1}{30}$, $\mu = 0.15$ and $\beta = \frac{1}{40}$.

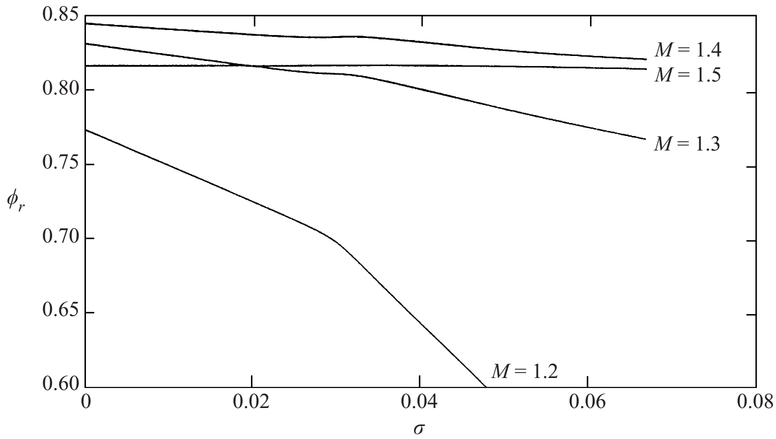

Figure 6. Variation of amplitude ratio ϕ_r with σ for different values of M, with $\alpha_h = 0.98$, $Q = 10$, $\mu = 0.15$ and $\beta = \frac{1}{40}$.

that for low β (e.g. $\beta < \frac{1}{50}$), the effect of Q decreases with increasing M, but for large β, the variation is not regular and depends upon the particular combination of M and $\beta_{\max}$ (i.e. terminating β) combination. In all the cases, the intermediate amplitude shows the least variation.

It seems that the presence of multi-ions produces only a small quantitative deviation in the parametric variations of a rarefactive solitary wave. Hence the effect remains quite small for a wide range of amplitudes, except for a sufficiently small-amplitude solution. However, for an appreciably large-amplitude (increasing-width) rarefactive solitary waves, the deviation starts to increase. From Table 1, we may recall that both L_h and H_l in these regions show trapping-like energy conditions, and may indicate an active participation of both species in the process of transition of rarefactive solitary waves into double layers. This may in turn enhance the deviation due to the presence of multi-ions.

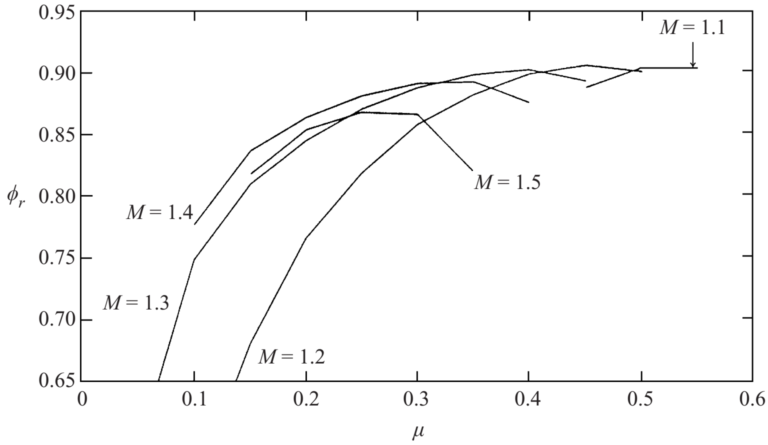

Figure 7. Variation of amplitude ratio ϕ_r with μ for different values of M, with $\alpha_h = 0.98$, $Q = 10$, $\sigma = \frac{1}{30}$ and $\beta = \frac{1}{40}$.

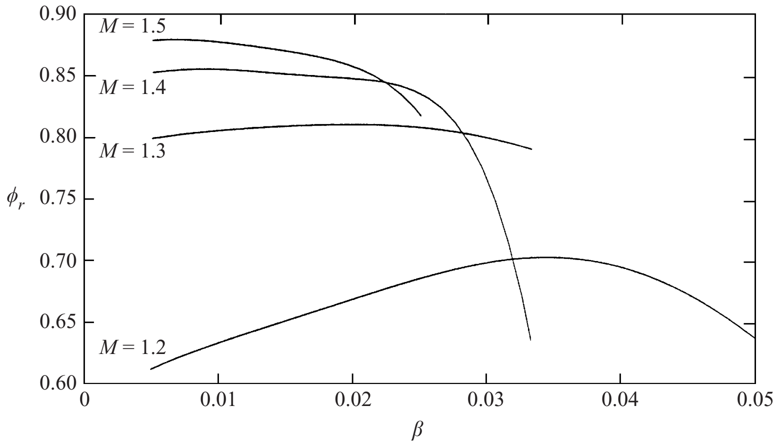

Figure 8. Variation of amplitude ratio ϕ_r with β for different values of M, with $\alpha_h = 0.98$, $Q = 10$, $\sigma = \frac{1}{30}$ and $\mu = 0.15$.

4. Conclusions

We have investigated in detail the effect of the multi-ion species on the parametric variation of a rarefactive solitary wave. The emphasis has been on the effect of the second ion species on the corresponding amplitude–width variations. It is found that the width variation depends crucially on the ion concentration α_h, and gives U-shaped profiles for changing concentrations. Hence, with increasing α_h (decreasing light-ion concentration), rarefactive solitary waves transform from region I to III, exhibiting anomalous width variation. Unlike α_h, the ion mass ratio Q produces only small quantitative changes, which is similar to what is observed due to ion temperature σ.

The energy–amplitude relations for ions (Table 1) indicate an enhancement in trapping-like processes for large-amplitude ('increasing-width'; region III) solutions involving ions with intermediate energies (i.e. low-energy heavy ions and high-energy light ions, represented by L_h and H_l respectively). This results in a transition

https://doi.org/10.1017/S0022377801001404 Published online by Cambridge University Press

of the large-amplitude solution to a double layer. This also seems to account for the observed increase in the multi-ion effect in the neighbourhood of double layers. Interestingly, the influence of the second ion species becomes most prominent for a single-to-multi-ion transition (small amplitude) and in the vicinity of double-layer-like solutions. In between these two extrema, it produces small quantitative deviations, which decrease with increasing amplitude.

It is well known that the amplitude of a compressive solitary wave is bounded by light-ion reflection (White et al. 1972; Tran 1979). Analogously, the trapping-like process seems to explain the reduction in amplitude in the case of rarefactive solitary waves. However, the latter is also bounded by the heavy-ion impurity for a large-amplitude solution.

Our analysis shows that the presence of a second ion species influences the rarefactive solitary-wave solution quite effectively. A more elaborate and complete investigation of the width–amplitude variation profile seems to be necessary for the understanding of the different nonlinear structures, namely rarefactive solitary waves and double layers, observed in the auroral plasma (Reddy et al. 1992). The phenomena of the increase in width with increasing amplitude for rarefactive solitary waves is quite likely to be observed in space plasmas, which we have already indicated in our previous work (Ghosh et al. 1996; Ghosh and Iyengar 1997b). A comparison of our theoretical investigations with experimental observations will be communicated elsewhere.

Acknowledgements

One of the authors, S. S. Ghosh, would like to thank CSIR for its Research Associateship for the completion of the work. The work was previously supported by The Asiatic Society, Calcutta under the scheme of The Meghnad Saha Research Fellowship, and the facilities were provided by the Director and the Plasma Physics Group of the Saha Institute of Nuclear Physics (SINP), Calcutta.

References

Baboolal, S., Bharuthram, R. and Hellberg, M. A. 1990 *J. Plasma Phys.* **44**, 1.

Berthomier, M., Pottelette, R. and Malingre, M. 1998 *J. Geophys. Res.* **103**, 4261.

Böstrom, R., Gustafsson, G., Holback, B., Holmgren, G., Koshkinen, H. and Kintner, P. 1988 *Phys. Rev. Lett.* **61**, 82.

Böstrom, R., Holback, B. and Holmgren, G. 1989 *Physica Scripta* **39**, 782.

Buti, B. 1983 *Astrophys. J.* **268**, 420.

Ghosh, S. S. and Iyengar, A. N. S. 1997a *Phys. Plasmas* **4**, 2139.

Ghosh, S. S. and Iyengar, A. N. S. 1997b *Phys. Plasmas* **4**, 3204.

Ghosh, S. S., Ghosh, K. K. and Iyengar, A. N. S. 1996 *Phys. Plasma* **3**, 3939.

Kadomtsev, B. B. 1992 *Tokamak Plasma: A Complex Physical System*. Bristol: Institute of Physics Publishing, p. 48.

Reddy, R. V., Lakhina, G. S. and Verheest, F. 1992 *Planet Space Sci.* **40**, 1055.

Tran, M. Q. 1979 *Physica Scripta* **20**, 317.

White, R. B., Fried, B. D. and Coroniti, F. V. 1972 *Phys. Fluids* **15**, 1484.